EXAFS Analysis with Self-consistent Atomic Potentials

Shelly D. Kelly and Bruce Ravel

Argonne National Laboratory, 9700 South Cass Avenue, Argonne, IL 60439

Abstract. Theoretical EXAFS spectra generated by FEFF6 and FEFF8 are compared. As a test of the effect of charge transfer on EXAFS analysis, we examine the aqueous uranyl (UO_2^{2+}) ion. We find that the major difference between FEFF8 and FEFF6 is the edge energy position of approximately 5 eV. Modest changes in the forward focusing multiple scattering path of the uranyl resulting with FEFF8 produce a better model of the measured hydrated uranyl spectrum.

Keywords: EXAFS, FEFF, Uranyl
PACS: 87.64.Fb

INTRODUCTION

Theoretical EXAFS spectra generated by FEFF6 have been used successfully for many years for the analysis of measured EXAFS spectra, on a wide variety of samples. FEFF8 introduces the self-consistent calculation of atomic potentials, allowing for charge transfer and a more accurate estimate of the X-ray absorption edge energy. As a test of the effect of charge transfer on EXAFS analysis, we examine the aqueous uranyl (UO_2^{2+}) ion. Like other actinides, U(VI) often exists as a uranyl moiety with two double-bonded axial oxygen (Oax) atoms in a rigid, nearly co-linear arrangement about uranium (Oax=U=Oax). The short bonding distance and the rigidity of the U=Oax bond result in significant multiple scattering contributions from the axial oxygen atoms in the U L_{III}-edge EXAFS spectrum. The short double bond, approximately 1.8 Å long, between the U atom with 92 electrons and the O atom with 8 electrons may be a challenge for the model of neutral, overlapped muffin tin potential used in FEFF6. Here we test the effect of self-consistent atomic potentials and charge transfer on the analysis of an aqueous uranyl EXAFS spectrum.

MATERIALS AND METHODS

Uranium L_{III}-edge spectra were collected at the MR-CAT 10-ID beamline [1] at the Advance Photon Source. The general beamline setup parameters are given elsewhere [2]. The measurements were made in quick-scanning mode of the monochromator.

The aqueous uranyl standard was prepared from stock solutions of 8 mM uranyl chloride. The solution was brought to approximately pH 2 by the addition of HCl. This low pH ensures that the major uranyl species is hydrated.

Several EXAFS spectra were aligned and then averaged to increase the signal-to-noise ratio. The background was removed by using Athena [3], an interface to IFEFFIT [4]. The background parameter Rbkg was set to 1.0 Å. The spectra were modeled by using FEFFIT from the UWXAFS package [5].

The FEFF calculation is based on the crystal structure of uranyl acetate [6]. Theoretical calculations were produced with FEFF6 and FEFF8 [7] with four different configurations each. The first configuration, *atomic*, uses one atomic potential for each atom type. The second configuration, *Oax/Oeq*, uses independent atomic potentials for the Oax atoms and the Oeq atoms. The third and fourth configurations apply automatic functions for overlapping potentials (AFOLP) to the first two configurations.

The EXAFS model of the hydrated uranyl contains five scattering paths of the photoelectron. The first is the single scattering (SS) path from the two Oax atoms (R = 1.8 Å) of the uranyl. The second SS path is from the six Oeq atoms (R = 2.4 Å) of the uranyl. The next three paths are multiple scattering (MS) paths of the linear Oax1=U=Oax2 moiety. The notation for the MS paths gives the Oax atoms as OaxA and OaxB. Each MS path has degeneracy of 2: one path with A and B of 1 and 2 and another path with A and B of 2 and 1. The first double scattering (MS) path is U-OaxA-U-OaxA-U. The second three-leg MS path is U-OaxA-OaxB-U. The third four-leg-focusing MS path is U-OaxA-U-OaxB-U. The EXAFS model includes independent ΔR, σ^2, and ΔE values for both SS U-Oax and U-Oeq paths. The MS paths are constrained in terms of the SS U-Oax path. The MS path lengths are

CP882, *X-ray Absorption Fine Structure—XAFS13*
edited by B. Hedman and P. Pianetta

twice the SS path length, and the ΔE value is the same as that for the SS path. The U-OaxA-U-OaxA MS path has a σ^2 value that is mathematically equivalent to 4 times the SS path. The U-OaxA-OaxB and U-OaxA-U-OaxB MS paths have σ^2 values between 2 times and 4 times that of the SS path. In the limit where the U atom with 92 electrons has minimal contribution to σ^2 (compared to the Oax atoms with 8 electrons), these MS paths have a σ^2 value twice that of the SS path. In this limit, we assume that the U atom is infinitely heavy, as compared to the Oax atoms.

TABLE 1. List of muffin tin radii (Rmn) and Norman radii (Rnm) for the different potentials within FEFF8 and FEFF6.

Potential	Oax/Oeq		Oax/Oeq AFOLP	
	Rmt	**Rnm**	**Rmt**	**Rnm**
		FEFF6		
Oax	0.824	1.045	0.824	1.045
Oeq	0.786	1.004	0.786	1.004
U	1.204	1.516	1.204	1.516
		FEFF8		
Oax	0.730	1.073	0.970	1.073
Oeq	0.689	1.032	0.929	1.032
U	1.038	1.507	1.367	1.507

RESULTS AND CONCLUSIONS

A comparison of the muffin tin radii and the Norman radii for the different potentials for FEFF6 and FEFF8 are shown in Table 1 for the Oax/Oeq potential models. The values for the atomic potential models are similar but are not shown. The Norman radii represent the radius in which the atomic charge density within the atom is equal to the atomic number Z. The muffin tin radii are determined such that the muffin tins of all atoms within the cluster just touch. Excess charge between the Norman radii and the muffin tin radii is given to the interstitial region in between the muffin tins. The AFOLP causes the muffin tin radii to be overlapped by 10–30%. The FEFF8 AFOLP potentials do not affect the muffin tin radii (Table 1), as charge is moved from the muffin tins in a self-consistent manner. The FEFF6 AFOLP potentials increase the muffin tin radii by approximately 20% (see Table 1).

TABLE 2. Charge transfer for FEFF8 calculations.

Pot.	Oax/Oeq	Oax/Oeq AFOLP	Atomic	Atomic AFOLP
Oax	-0.257	-0.254	-0.292	-0.292
Oeq	-0.254	-0.254		
U	1.014	1.014	0.990	0.990

The amount of charge transfer for the Oax, Oeq, and U potentials, as determined by FEFF8 calculations, are listed in Table 2. The results show little difference for the different atomic potentials, with ~ -0.25 to -0.30 electrons transferred from the O atoms and ~ 1 electron transferred to the U atom.

TABLE 3. EXAFS results for hydrated uranyl spectra modeled with FEFF6 and FEFF8 using different atomic models.

Model	R (Å)	σ^2 (10^{-3} Å^2)	ΔE (eV)	RCS
		2 U-Oax, FEFF6		
Atomic	1.76(1)	1.1(4)	-0.4(14)	105
Atomic	1.76(1)	1.4(4)	0.6(14)	109
AFOLP				
Oax/Oeq	1.76(1)	1.1(4)	-0.4(14)	105
Oax/Oeq	1.76(1)	1.1(4)	-0.4(14)	114
AFOLP				
		6 U-Oax		
Atomic	2.42(1)	8.1(8)	2.9(9)	
Atomic	2.42(1)	9.5(9)	3.2(10)	
AFOLP				
Oax/Oeq	2.42(1)	8.1(8)	2.9(9)	
Oax/Oeq	2.41(1)	9.1(9)	2.8(10)	
AFOLP				
		2 U-Oax, FEFF8		
Atomic	1.76(1)	0.9(4)	-1.1(12)	89
Atomic	1.76(1)	0.9(4)	-1.1(12)	88
AFOLP				
Oax/Oeq	1.76(1)	0.8(4)	-1.3(11)	97
Oax/Oeq	1.76(1)	0.8(4)	-1.3(11)	96
AFOLP				
		6 U-Oeq		
Atomic	2.42(1)	8.7(8)	1.8(9)	
Atomic	2.42(1)	8.7(8)	1.8(9)	
AFOLP				
Oax/Oeq	2.42(1)	8.6(8)	1.5(8)	
Oax/Oeq	2.42(1)	8.6(8)	1.5(8)	
AFOLP				

A comparison of the FEFF6 and FEFF8 calculations for each path of the hydrated uranyl spectrum is shown in Figure 1. This comparison uses zero for all the EXAFS parameters, except that S_0^2 was set to 1. The SS paths are similar beyond a ~ 5-eV shift in the edge energy (as shown by the difference at low k in the χ(k) spectrum). The largest difference between the FEFF6 and FEFF8 calculations is the change in shape and amplitude of the four-leg focusing path U-OaxA-U-OaxB.

To properly align the EXAFS spectra to the theory, a different E_0 values in the background removal step were selected for the models based on FEFF6 and FEFF8. The minor differences in the resulting χ(k) spectra at low wave numbers are shown in Figure 2. A test using the same χ(k) spectra for both the FEFF8 and FEFF6 resulted in no change in the final

parameters but larger than desirable energy shift values. The typical U-Oax resonance feature of the XANES region of the EXAFS spectra is shown at 2-3 $Å^{-1}$ in the $\chi(k)$ spectra. By allowing the model to have two different energy shift parameters for the Oax and the Oeq paths, we were able to model the spectrum from 2.5 $Å^{-1}$. With only one energy shift parameter, the spectrum from ~ 3.3 $Å^{-1}$ can be modeled with little difference in the modeling parameters. The difference in the Oax and Oeq energy shift values for both the FEFF8 and FEFF6 calculations are similar, at approximately 3 eV.

EXAFS models based on the four different potentials for each version of FEFF show similar best-fit values (Table 3) for the SS Oax and SS Oeq paths. The three MS paths included in the models exclude any new parameters (as described earlier). The reduced-chi-square (RCS) values are also in Table 3. The decrease of ~ 20% in RCS shows that the FEFF8 calculations are modestly more accurate than FEFF6 at reproducing the MS contribution to the EXAFS spectrum. We speculate that FEFF8 may give more reliable results for EXAFS spectra from uranyl spiecies with another unknown signal, such as a bidentate C or P, in the U-Oax MS region.

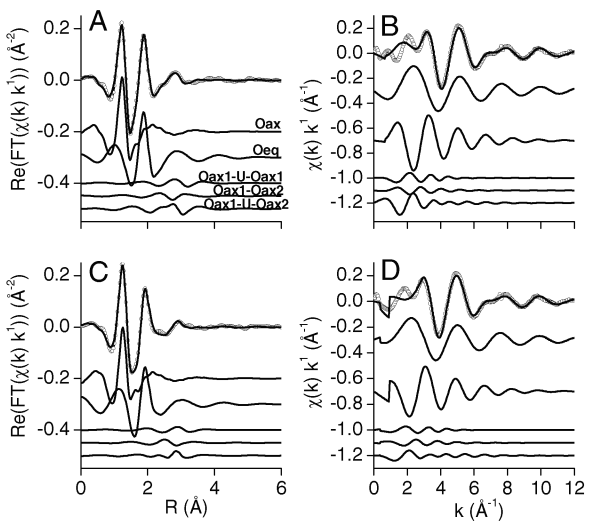

FIGURE 2. The real part of the Fourier transform (A and C) and the EXAFS spectra (B and D) of the hydrated uranyl EXAFS spectrum (top: symbol) and Model-fit (top: line). The top and bottom rows show the FEFF8 and FEFF6 models based on the Oax/Oeq AFOLP. The components of the model are offset below. Data range is from 2.5 to 12 $Å^{-1}$, and the fit range is from 1 to 3.3 Å.

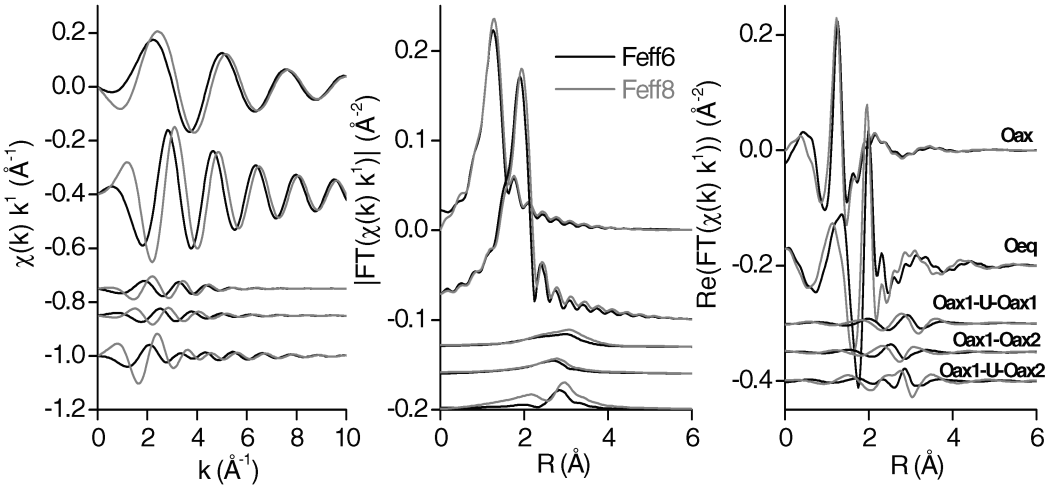

FIGURE 1. A comparison of the EXAFS spectra calculated by FEFF6 and FEFF8 using the Oax/Oeq AFOLP.

ACKNOWLEDGEMENTS

Our work is supported by the ERSD-BER, Office of Science (OS), Department of Energy (DOE), under contract W-31-109-Eng-38. Work at the APS is supported by the DOE-OS, Office of Basic Energy Sciences. MRCAT operations are supported by DOE and MRCAT member institutions.

REFERENCES

1. C U Segre, N E Leyarovska, L D Chapman et al., *Synchrotron Rad. Inst.* **CP521**, 419 (2000).
2. S. D. Kelly, K. M. Kemner, J. B. Fein et al., *Geochim. Cosmochim. Acta.* **66** (22), 3855 (2002).
3. B. Ravel and M. Newville, *J. Synch. Rad.* **12** (4), 537 (2005).
4. M Newville, J. Synch. Rad. **8**, 322 (2001).
5. E A Stern, M Newville, B Ravel et al., *Physica B* **208 & 209**, 117 (1995).
6. D Templeton, A Zalkin, H Ruben et al., *Acta Cryst.* **C41**, 1439 (1985).
7. S I Zabinsky, J J Rehr, A Ankudinov et al., *Phys. Rev. B* **52** (4), 2995 (1995).